

**ACTIVE VIBRATION CONTROL TO ATTENUATE HAND-
ARM VIBRATION FOR ORBITAL SANDER**

AHMAD ZHAFRAN BIN AHMAD MAZLAN

2012

**ACTIVE VIBRATION CONTROL TO ATTENUATE HAND-ARM
VIBRATION FOR ORBITAL SANDER**

by

AHMAD ZHAFRAN BIN AHMAD MAZLAN

Thesis submitted in fulfilment of the requirements

for the degree of

Master of Science

October 2012

DECLARATION

I hereby declare that the work reported in this thesis is the result of my own investigation and that no part of the thesis has been plagiarized from external sources. Materials taken from other sources are duly acknowledged by giving explicit references.

Signature:

Name of student: AHMAD ZHAFRAN BIN AHMAD MAZLAN

Matrix number: P-CM0320

Date: 4 October 2012

ACKNOWLEDGEMENTS

First of all, my highness praises and all thanks to Almighty Allah Subhanahu Wataalla, the Most Gracious the Most Merciful, who gives me the patience, knowledge and courage to complete this research.

I would like to express my sincere gratitude to my research supervisor, Prof. Dr. Zaidi bin Mohd Ripin, who gives me a constant encouragement, good guidance and suggestions all the way of this research. Without him, this research will not be the same as presented here.

I also want to extend my gratitude to the technicians especially Mr. Wan Mohd Amri bin Wan Mamat Ali, who always work with me for the experimental works. Apart of that, I want to thank to all my fellow friends from the Vibration Laboratory whose give their help, moral support, and some valuable hints for completing my research.

Beside that, I am gratitude to Kementerian Pengajian Tinggi Malaysia and Universiti Sains Malaysia for awarding me Skim Latihan Akademik Bumiputera (SLAB) scholarship which assisted my financial.

Last but not least, I would like to express my deepest gratitude to my wife, Mrs. Fauziah binti Abdullah, my children; Iqbal Zayyaan and Iqbal Rizqin, and my whole family for their kindly love and continuous support during my intricate times in completing this research.

AHMAD ZHAFRAN BIN AHMAD MAZLAN

October 2012

TABLE OF CONTENTS

	Page
ACKNOWLEDGEMENTS	ii
TABLE OF CONTENTS	iii
LIST OF TABLES	vii
LIST OF FIGURES	viii
LIST OF SYMBOLS	xii
LIST OF NOTATIONS	xvi
LIST OF APPENDICES	xviii
LIST OF PUBLICATIONS	xviii
ABSTRAK	xix
ABSTRACT	xx
CHAPTER 1: INTRODUCTION	1
1.1 Background study	1
1.2 Problem statement	3
1.3 Motivation of the work	4
1.4 Objectives	4
1.5 Scope	4
1.6 Thesis outlines	5
CHAPTER 2: LITERATURE REVIEW	6
2.1 Overview	6
2.2 Hand-arm vibration syndrome (HAVs) and the epidemiological studies	6
2.3 The guidelines to protect and measure hand-arm vibration	8
2.3.1 Guidelines and references for hand-transmitted vibration	8

2.3.2	Standard measurement of hand-transmitted vibration	9
2.4	Modeling of hand-held power tools	12
2.5	Human hand-arm biodynamic models	13
2.5.1	To-the-hand biodynamic models	13
2.5.2	Through-the-hand biodynamic models	15
2.6	Coupled power tool-hand-arm models	15
2.7	Attenuation of hand-transmitted vibration	16
2.7.1	Vibration isolation approaches	17
2.7.2	Vibration absorption approaches	19
2.7.3	Active vibration control (AVC) approaches	20
2.7.3.1	Active force control (AFC) technique	23
2.8	Discussion	24
2.9	Summary	27
	CHAPTER 3: METHODOLOGY	28
3.1	Overview	28
3.2	Orbital sander specification and description	28
3.3	Determination of the sensor and actuator locations	30
3.4	Measurement of the input spectrum	31
3.4.1	Free-free condition	31
3.4.2	The operating condition	31
3.5	Experimental modal analysis	33
3.6	Model development and verification	34
3.6.1	Modal mass, stiffness and damping	35
3.6.2	Modal parameters	36
3.6.3	Model validation	37

3.7	Mathematical model of the orbital sander	38
3.7.1	Matlab coding development	39
3.7.2	Simulink diagram development	41
3.8	Model of active vibration control (AVC) system for the orbital sander	43
3.8.1	Active system with PID controller	44
3.8.1.1	Simulink diagram development	46
3.8.2	Active system with PID+AFC controller	47
3.8.2.1	Simulink diagram development	49
3.9	Disturbances	51
3.10	Mathematical model of the hand-arm system	51
3.10.1	Simulink diagram development	53
3.11	Development of the coupled orbital sander-hand-arm model	54
3.11.1	Simulink diagram development	55
3.12	Summary	57
	CHAPTER 4: RESULTS AND DISCUSSION	58
4.1	Overview	58
4.2	Input spectrum result of the orbital sander	58
4.2.1	Free-free condition	58
4.2.2	The operating condition	60
4.3	Experimental modal analysis	66
4.3.1	Modes of vibration in the z -axis direction	66
4.4	Model validation	70
4.5	Simulation result of the orbital sander	73
4.5.1	Matlab and Simulink results	73

4.5.2	Comparison of the simulation result	75
4.6	Simulation result of the active system	76
4.6.1	Tuning of the PID controller	77
4.6.2	Tuning of the AFC controller	79
4.7	Performance evaluation	81
4.7.1	Performance of the orbital sander model using various control schemes	81
4.7.2	Performance of the coupled orbital sander-hand-arm model	83
4.7.3	Performance of the system with the presence of external disturbance	85
CHAPTER 5: CONCLUSION		88
5.1	Conclusion	88
5.2	Recommendation for future work	89
REFERENCES		90
APPENDICES		98
Appendix A: Hand-arm vibration reference chart		98
Appendix B: Mathematical model of the orbital sander (Matlab coding)		99
Appendix C: Mathematical model of the passive and active systems of the orbital sander (Simulink digram)		101
Appendix D: Overall mathematical model of coupled orbital sander-hand-arm model (Simulink diagram)		103
Appendix E: Model and simulation parameters (Matlab and Simulink)		107
Appendix F: Performance of coupled orbital sander-hand-arm model with various control schemes		108
PUBLICATIONS		111

LIST OF TABLES

	Page
1.1 The literatures of the high vibration level power tools	1
3.1 Technical data Bosch GSS 230 Professional Orbital Sander	30
3.2 Reynolds and Soedel, (1972) single-degree-of-freedom model parameters in the x_h , y_h and z_h -axis direction ($f > 100$ Hz) (Rakheja, et al., 2002)	52
3.3 Parts and its function in the Simulink diagram	57
4.1 Output acceleration of front and rear handle in the three axes (x , y and z -axis) with various push forces	63
4.2 Frequency-weighted acceleration of the orbital sander front handle in the three axes with various push forces	65
4.3 Compact mode complexity for z -axis direction of the orbital sander	68
4.4 Modal mass, stiffness and damping for the orbital sander	70
4.5 Comparison of acceleration output for the orbital sander model using various control schemes	83
4.6 Comparison of acceleration output for the coupled orbital sander-hand-arm model using various control schemes	85
4.7 Acceleration output of the orbital sander and the coupled orbital sander-hand-arm model in two different conditions using various control schemes	87

LIST OF FIGURES

	Page
2.1 The example of Vibration White Finger (VWF) disease (Hunter, 2011)	7
2.2 Biodynamic and basicentric coordinate system for flat-palm position (ISO 5349-1, 2001)	10
2.3 Frequency-weighting filter (W_h) with band limitation for hand-transmitted vibration (ISO 5349-1, 2001)	11
2.4 Cross section diagram and dynamic model of pneumatic hammer (Golysheva, et al., 2004)	12
2.5 Anti-vibration glove used to attenuate hand-arm vibration when using the orbital sander (Lee Valley, 2012)	18
2.6 Anti-vibration side handle (Makita, 2012a)	19
2.7 Basic control diagram for AVC system (Stienecker, 2011)	21
3.1 The flow chart of overall approach of this research	29
3.2 Bosch GSS 230 Professional Orbital Sander	28
3.3 Orbital sander free-free condition experiment set-up with detail view of tri-axial accelerometer (B&K 4506)	31
3.4 Signal analyzer device (iMC, cs-8008) and dynamometer amplifier (Kistler, type 9272)	32
3.5 Measurement set-up of the orbital sander input spectrum	32
3.6 Orbital sander geometry modeling in LMS software	33
3.7 Experimental set-up for impact testing	34
3.8 A three-degree-of-freedom modal model of the orbital sander	38
3.9 Full Simulink diagram of the passive system of the orbital sander	42
3.10 Shear actuator to be used for AVC system ($A=B=10$ mm, $L=23$ mm) (Physik Instruments, 2009b)	44
3.11 Full Simulink diagram of the active system with PID controller for the orbital sander	47

3.12	The overall dynamic system with an input of AFC technique	49
3.13	Full Simulink diagram of active system with PID+AFC controller for the orbital sander	50
3.14	A single-degree-of-freedom hand-arm model	52
3.15	Full Simulink diagram of the passive system of the hand-arm model	53
3.16	Model of the coupled orbital sander-hand-arm with AVC system	55
3.17	Full Simulink diagram of the active system with PID+AFC controller for the coupled orbital sander-hand-arm model	56
4.1	The FFT of the acceleration in the x , y and z -axis direction of the orbital sander front handle when in the free-free condition	59
4.2	The FFT of the acceleration in the x , y and z -axis direction of the orbital sander rear handle when in the free-free condition	59
4.3	The push force (internal disturbance, F) graph in z -axis direction when operating the orbital sander (time domain)	61
4.4	The FFT graph of the push force (internal disturbance, F) in the z -axis direction when operating the orbital sander	62
4.5	The FFT of the acceleration in the x , y and z -axis of the orbital sander front handle when sanding with 22.7 N of push force	63
4.6	The comparison of output acceleration in the x , y and z -axis direction of the front and rear handle with various sanding push force	64
4.7	The comparison of frequency-weighted acceleration in the x , y and z -axis of the orbital sander front handle with various sanding push forces	65
4.8	The FRF graph of the experimental modal analysis in the z -axis direction of the orbital sander with "Polymax" function	67
4.9	Comparison of modal assurance criterion (MAC) between each mode of the orbital sander in the z -axis direction	69
4.10	Mode deflection shapes of the orbital sander in z -axis direction	69
4.11	The validation of FRF graph between experiment and model of the orbital sander (acceleration)	71
4.12	The comparison of acceleration output $A(\omega)$ between experiment	72

	and model of the orbital sander	
4.13	The output acceleration of the orbital sander when subjected to the input force as in Figure 4.3 (time domain)	74
4.14	The output acceleration of the orbital sander when subjected to the input force as in Figure 4.3 (frequency domain)	74
4.15	The comparison of acceleration output between simulation and actual experiment result of the orbital sander (time domain)	75
4.16	The comparison of acceleration output between simulation and actual experiment result of the orbital sander (frequency domain)	76
4.17	Displacement result for different values of K_P and K_D with a step input reference signal for the PD scheme	78
4.18	Error signals for different values of K_P and K_D with a step input reference signal for the PD scheme	78
4.19	Displacement result for different values of estimated masses (M^*) with a step input reference signal for the PD+AFCCA scheme	79
4.20	Error signals of estimated masses ($M^*=0.8$ kg) with a step input reference signal for the PD+AFCCA scheme	80
4.21	Comparison of acceleration output between passive, PD and PD+AFCCA model for the orbital sander (time domain)	82
4.22	Comparison of acceleration output between passive, PD and PD+AFCCA model for the orbital sander (frequency domain)	82
4.23	Comparison of acceleration effect on the hand-arm system between passive, PD and PD+AFCCA model for the orbital sander (time domain)	84
4.24	Comparison of acceleration effect on the hand-arm system between passive, PD and PD+AFCCA model for the orbital sander (frequency domain)	84
4.25	Acceleration output of the orbital sander and the coupled orbital sander-hand-arm model in two different conditions using various control schemes	87
A.1	Hand-arm vibration quick reference chart (HSC, 2005)	98
C.1	Simulink diagram of the m_1 subsystem of the orbital sander	101
C.2	Simulink diagram of the m_2 subsystem of the orbital sander	102

C.3	Simulink diagram of the m_3 subsystem of the orbital sander	102
D.1	Full Simulink diagram of the passive system of coupled orbital sander-hand-arm model	103
D.2	Full Simulink diagram of the active system of coupled orbital sander-hand-arm model with PID controller	104
D.3	Simulink diagram of the m_1 subsystem of the coupled orbital sander-hand-arm	105
D.4	Simulink diagram of the m_2 subsystem of the coupled orbital sander-hand-arm	105
D.5	Simulink diagram of the m_3 subsystem of the coupled orbital sander-hand-arm	106
D.6	Simulink diagram of the m_h subsystem of the coupled orbital sander-hand-arm	106
F.1	Comparison of acceleration output between passive, PD and PD+AFCCA with an external disturbance (time domain)	108
F.2	Comparison of acceleration output between passive, PD and PD+AFCCA with an external disturbance (frequency domain)	109
F.3	Comparison of acceleration effect on the hand-arm system between passive, PD and PD+AFCCA with an external disturbance (time domain)	110
F.4	Comparison of acceleration effect on the hand-arm system between passive, PD and PD+AFCCA with an external disturbance (frequency domain)	110

LIST OF SYMBOLS

Symbols	Descriptions	Unit
$A(\omega)$	Calculated acceleration	m/s^2
$A(8)$	Daily vibration exposure based on reference period of 8 hours	m/s^2
A_i	A scaling constant for the i^{th} mode	-
a_{hv}	Total frequency-weighted acceleration	m/s^2
a_{hwx}	Overall weighted RMS acceleration in x -axis	m/s^2
a_{hwy}	Overall weighted RMS acceleration in y -axis	m/s^2
a_{hwz}	Overall weighted RMS acceleration in z -axis	m/s^2
$[C]$	(DOFs by DOFs) Damping matrix	kg/s
c_a	Damping of the piezo actuator	kg/s
c_h	Damping of the hand-arm system	kg/s
c_i	Modal damping at each mode (i)	kg/s
c_1	Modal damping 1 of the orbital sander	kg/s
c_2	Modal damping 2 of the orbital sander	kg/s
c_3	Modal damping 3 of the orbital sander	kg/s
$[c_i]$	(Modes by modes) Modal damping matrix	kg/s
$D(s)$	Denominator of orbital sander transfer function	-
$D_1(s)$	Numerator 1 of the orbital sander transfer function	-
$D_2(s)$	Numerator 2 of the orbital sander transfer function	-
$D_3(s)$	Numerator 3 of the orbital sander transfer function	-
$e(t)$	Error signal	m
$E(s)$	Transfer function error signal	m
$F(s)$	Complex quantity of input force	N

F	Internal disturbance of the orbital sander	N
F^*	Estimated disturbance force	N
F_a	Force of the piezo actuator	N
F_e	External disturbance of the orbital sander	N
F_a^*	Total force of the piezo actuator	N
$G_c(s)$	PID controller transfer function	-
$H(\omega)$	Transfer function/ FRF of the orbital sander	$(m/s^2)/N$
i^{th}	Modes	-
$[K]$	(DOFs by DOFs) Stiffness matrix	N/m
K_D	Derivative gain	-
K_I	Integrator gain	-
K_P	Proportional gain	-
k_a	Stiffness of the piezo actuator	N/m
k_h	Stiffness of the hand-arm system	N/m
k_i	Modal stiffness at each mode (i)	N/m
k_1	Modal stiffness 1 of the orbital sander	N/m
k_2	Modal stiffness 2 of the orbital sander	N/m
k_3	Modal stiffness 3 of the orbital sander	N/m
$[\cdot\cdot k \cdot\cdot]$	(Modes by modes) Modal stiffness matrix	N/m
L	Shear piezo actuator thickness	mm
$[M]$	(DOFs by DOFs) Mass matrix	kg
M^*	Estimated mass	kg
m_a	Mass of the piezo actuator	kg
m_h	Mass of the hand-arm system	kg
m_i	Modal mass at each mode (i)	kg

m_1	Modal mass 1 of the orbital sander	kg
m_2	Modal mass 2 of the orbital sander	kg
m_3	Modal mass 3 of the orbital sander	kg
$[\cdot m \cdot]$	(Modes by modes) Modal mass matrix	kg
(r)	Correlation coefficient	-
$r(t)$	Reference output	m
$[r(i)]$	(DOFs by DOFs) Residue matrix for the i^{th} mode	-
s	Complex number in magnitude and phase	-
T	Total daily vibration exposure	h
T(s)	Complex quantity of vibration transmissibility	-
T_0	Reference duration of 8 hours	h
$\{u_k\}$	Mode shape of the i^{th} mode	-
$\{u_k\}^t$	Transpose mode shape of the i^{th} mode	-
W_h	Frequency-weighting filter	-
ω_i	Damped natural frequency of the i^{th} mode	Hz
X(s)	Complex quantity of resulting displacement	m
$X_0(s)$	Complex quantity of excitation displacement	m
$\dot{X}(s)$	Complex quantity of resulting velocity	m/s
$\dot{X}_0(s)$	Complex quantity of excitation velocity	m/s
$\ddot{X}(s)$	Complex quantity of resulting acceleration	m/s^2
$\ddot{X}_0(s)$	Complex quantity of excitation acceleration	m/s^2
$Z_a(s)$	Resulting displacement of the piezo actuator transfer function	m
$Z_D(s)$	Complex quantity of DPMI	$\text{N}/(\text{m/s}^2)$
z_a	Resulting displacement of the piezo actuator	m
z_e	Experimental FRF data	$(\text{m/s}^2)/\text{N}$

z_h	Resulting displacement of the hand-arm system	m
z_i	Resulting displacement of i^{th} modal mass of the sander	m
z_m	Model FRF data	$(\text{m/s}^2)/\text{N}$
z_1	Resulting displacement of modal mass 1 of the orbital sander	m
z_2	Resulting displacement of modal mass 2 of the orbital sander	m
z_3	Resulting displacement of modal mass 3 of the orbital sander	m
\dot{z}_a	Resulting velocity of the piezo actuator	m/s
\dot{z}_h	Resulting velocity of the hand-arm system	m/s
\dot{z}_1	Resulting velocity of modal mass 1 of the orbital sander	m/s
\dot{z}_2	Resulting velocity of modal mass 2 of the orbital sander	m/s
\dot{z}_3	Resulting velocity of modal mass 3 of the orbital sander	m/s
\ddot{z}_a	Resulting acceleration of the piezo actuator	m/s^2
\ddot{z}_h	Resulting acceleration of the hand-arm system	m/s^2
\ddot{z}_1	Resulting acceleration of modal mass 1 of the orbital sander	m/s^2
\ddot{z}_2	Resulting acceleration of modal mass 2 of the orbital sander	m/s^2
\ddot{z}_3	Resulting acceleration of modal mass 3 of the orbital sander	m/s^2
\bar{z}_e	Average value of all experimental FRF data	$(\text{m/s}^2)/\text{N}$
\bar{z}_m	Average value of all model FRF data	$(\text{m/s}^2)/\text{N}$
σ_i	Damping coefficient of the i^{th} mode	kg/s
$[\Phi]$	(DOFs by modes) Mode shape matrix	-
$[\Phi]^t$	(DOFs by modes) Transpose mode shape matrix	-

LIST OF NOTATIONS

Symbols	Descriptions
AFC	Active Force Control
AFCCA	Active Force Control with Crude Approximation
AVC	Active Vibration Control
B&K	Bruel and Kjaer
CEACS	Combined Energy and Attitude Control System
CTS	Carpal Tunnel Syndrome
DPMI	Dynamic-point Mechanical Impedance
DVA	Dynamic Vibration Absorber
EAV	Exposure Action Value
ELV	Exposure Limit Value
EU	European Union
FE	Finite Element
FFT	Fast Fourier Transform
FL	Fuzzy Logic
FRF	Frequency Response Function
GA	Genetic Algorithm
HAVs	Hand-arm Vibration Syndrome
HSC	Health and Safety Commission
ILM	Iterative Learning Method
ISO	International Standardization Organization
LQG	Linear Quadratic Gaussian
MAC	Modal Assurance Criterion
MDOF	Multi-degree-of-freedom

MP	Mode Participant
NIWF	National Institute of Working Life
NN	Neural Network
OPERC	Off-highway Plant and Equipment Research Centre
PID	Proportional-integral-derivative
PD	Proportional-derivative
RMS	Root Mean Squares
R&S	Reynolds and Soedel
SDOF	Single-degree-of-freedom
TVA	Tuned Vibration Absorber
VWF	Vibration White Finger

LIST OF APPENDICES

	Page
A Hand-arm vibration reference chart	98
B Mathematical model of the orbital sander (Matlab coding)	99
C Mathematical model of the passive and active systems of the orbital sander (Simulink digram)	101
D Overall mathematical model of coupled orbital sander-hand-arm model (Simulink diagram)	103
E Model and simulation parameters (Matlab and Simulink)	107
F Performance of coupled orbital sander-hand-arm model with various control schemes	108

LIST OF PUBLICATIONS

	Page
1 Development of active vibration control cancellation pad for orbital sander	112

KAWALAN GETARAN AKTIF UNTUK MELEMAHKAN GETARAN TANGAN UNTUK MESIN PENGGILAP ORBIT

ABSTRAK

Penggunaan mesin penggilap orbit yang berterusan pada tahap getaran yang tinggi boleh menyumbang kepada sindrom getaran tangan. Untuk mengkaji pengurangan getaran tangan apabila menggunakan mesin penggilap orbit, analisis dinamik bagi mesin penggilap orbit telah dilakukan dengan menggunakan model pasangan mesin penggilap orbit dan tangan tertakluk kepada pad kawalan getaran aktif. Mesin penggilap orbit telah direka sebagai satu sistem dengan tiga darjah kebebasan di mana nilai-nilai bagi ragaman jisim, kekakuan dan redaman diperolehi daripada eksperimen analisis ragaman dan model Reynolds dan Soedel dengan darjah kebebasan tunggal telah dipilih untuk dijadikan model tangan. Pelbagai skim kawalan telah digunakan di dalam sistem kawalan getaran aktif termasuklah teknik kawalan terbitan berkadar dan kawalan daya aktif. Parameter reka bentuk yang dianalisis termasuklah lokasi penderia dan penggerak dan juga penggunaan model. Dua jenis gangguan telah dikenakan pada sistem di mana gangguan pertama di ukur semasa mengendalikan mesin penggilap orbit manakala gangguan kedua telah direka sebagai gelombang sinus untuk menguji tahap keberkesanan skim-skim kawalan yang telah digunakan. Keputusan simulasi menunjukkan bahawa skim kawalan yang menggunakan teknik kawalan daya aktif menghasilkan keputusan yang lebih baik walaupun di bawah pengaruh gangguan luar dengan pengurangan getaran tangan sebanyak 99.20 % berbanding dengan skim kawalan terbitan berkadar yang mengurangkan getaran tangan sebanyak 88.36 %. Keputusan ini juga membuktikan bahawa kawalan getaran aktif merupakan teknik yang efisien untuk mencapai getaran tangan yang rendah pada mesin penggilap orbit.

ACTIVE VIBRATION CONTROL TO ATTENUATE HAND-ARM VIBRATION FOR ORBITAL SANDER

ABSTRACT

Prolonged use of the orbital sander with high vibration level can lead to the hand-arm vibration syndrome (HAVs). In order to evaluate the attenuation of the hand-arm vibration when using the orbital sander, dynamic analysis of the orbital sander is carried out using coupled orbital sander-hand-arm model subjected to the active vibration control (AVC) pad. The orbital sander is modelled as a three-degree-of-freedom system where the values of the modal mass, stiffness and damping are derived from the experimental modal analysis and the single-degree-of-freedom of Reynolds and Soedel model is chosen to represent the hand-arm system. Various control schemes are applied in the AVC system including proportional-derivative (PD) and active force control (AFC) techniques. The design parameters analyzed include the sensor and the actuator locations and the modelling approach. Two disturbances are created for the system where the first disturbance is measured from the orbital sander operating condition and the second disturbance is modelled as a sine wave to test the robustness of the control schemes. The simulation result shows that the control scheme with AFC input produces a superior result even though under the influence of external disturbance with a reduction of 99.20 % of hand-arm vibration compared to the classical PD controller which reduces only 88.36 % of hand-arm vibration. The results also proved that the AVC pad is an effective way of achieving a low hand-arm vibration for the orbital sander.

CHAPTER 1

INTRODUCTION

1.1 Background study

Prolonged use of the power tools with high vibration level may expose the workers to the hand-arm vibration syndrome (HAVs). This syndrome is an association of the vascular and nonvascular disorder in the human hand-arm system (Bovenzi, 1998; Mansfield, 2005).

Researchers have evaluated the vibration level (frequency-weighted acceleration) of several power tools such as orbital sander, rock drill, pneumatic hammer and grass trimmer. The result shows that all these tools produced a high level of vibration. The detail of the literatures and the evaluated power tools are shown in Table 1.1.

Table 1.1: The literatures of the high vibration level power tools

Power tools	Weighted acceleration (a_{hv})	Researchers
Orbital sander	3.9 ~ 7.3 m/s^2	(Cherian, et al., 1996; Bovenzi, et al., 2005; Ko, 2008)
Rock drill	24 ~ 25 m/s^2	(Niekerk, et al., 1998; Oddo, et al., 2004)
Pneumatic hammer	30 m/s^2	(Golysheva, et al., 2004)
Grass trimmer	4.5 ~ 11.3 m/s^2	(Ko, et al., 2011a; Ko, et al., 2011b)

International Organization of Standardization (ISO) has produced two documentations which is ISO 5349-1 (2001) and ISO 5349-2 (2001) for evaluating the hand-transmitted vibration of the power tools. The European Union (EU) has set a vibration limit values of 2.5 m/s^2 for the Exposure Action Value (EAV) and 5 m/s^2 for the Exposure Limit Value (ELV) for daily vibration exposure A(8) (EU, 2002).

In order to observe the biodynamic response of the coupled power tool-hand-arm system, researchers have developed models of the hand-held power tools. Oddo, et al, (2004) and Golysheva, et al., (2004) developed the model of rock drill suspended handle and pneumatic hammer, respectively. The developed models can be used for the advance simulation of the system such as the addition of the control elements (Hassan, et al., 2010).

Rakheja, et al., (2002) carried out a comprehensive study of the biodynamic hand-arm models including to-the-hand and through-the-hand models in the study of dynamic-point mechanical impedance (DPMI) of the hand-arm system and the response of specific hand-arm segment due to the transmitted vibration. From the study, there are only three models; Reynolds and Soedel, (1972), Mishoe and Suggs, (1977) and Miwa, et. al., (1979), which obtained all the natural frequencies in the range of the formulated frequency and only Reynolds and Soedel, (1972) specified the range of frequency for each direction of the hand-arm model parameters.

There are two methods of modeling the couple of power tools with the hand-arm models, depending on the way the tool is handle which is directly in contact with the hand (Oddo, et al, 2004) or when some intercession material is added in between (Golysheva, et al., 2004; Ko, 2008). The direct coupling requires the use of four-pole parameters (Showdown, 1971) to extract the element characteristics between the tools and the hand-arm models. The second method is by modeling the structure of the intercession device between the tools and the hand-arm models.

In order to attenuate the hand-transmitted vibration from the power tools, various techniques are used to control the hand-transmitted vibration including passive and active control techniques. Passive control involves structural modification, vibration isolation and vibration absorption approaches (Golysheva, et

al., 2004). For cases where the disturbances of the dynamic system vary with time, passive control becomes ineffective and active vibration control (AVC) has to be introduced to the system (William, 2007; Hassan, et al., 2010).

There are various kinds of controller scheme which can be applied in AVC system to suppress the vibration of the tools such as proportional-integral-derivative (PID), neural network (NN), fuzzy logic (FL) and etc. Active force control (AFC) is one of the most effective technique in reducing the vibration for AVC system. For example, Hassan, et al, (2010) in his simulation work proved that AFC is better than other control techniques in suppressing the vibration of the hedge trimmer handle. This technique has also been used in robotics (Kwek, et al., 2003; Mailah, et al., 2009), automotive (Mohamad, 2004; Priyandoko, et al., 2009; Rajeswari and Lakshmi, 2010), aerospace (Varatharajoo, et al., 2011) and beam applications (Karagulle, et al., 2004; Knot, et al., 2011).

In this work, the hand-arm coupled with an orbital sander model is developed. Then, an active vibration control with various control techniques is included in the system and its efficacy is compared and evaluated.

1.2 Problem statement

Orbital sander is one of the power tools which produces high vibration level ($a_{hv} = 7.3 \text{ m/s}^2$) and exceed both EAV and ELV values set by EU, (2002). The passive control solutions are not fully effective in attenuating the hand-arm vibration for the orbital sander. Active vibration control (AVC) is one of the methods that can be used to improve the attenuation of the hand-arm vibration. The effectiveness of using the AVC pad in attenuating the hand-arm vibration level due to the use of the orbital sander is studied and evaluated in this work.

1.3 Motivation of the work

The applications of the active vibration control (AVC) technique to attenuate the vibration level of the power tools are rarely being studied. Also, there are no studies of using the AVC pad approaches to reduce the hand-arm vibration for the couple orbital sander-hand-arm system. These reasons have motivated this work.

1.4 Objectives

In this research, four objectives are set to be achieved:

- To carry out vibration analysis of the orbital sander
- To develop coupled orbital sander-hand-arm model
- To attenuate hand-arm vibration for the orbital sander using active vibration control (AVC) pad
- To compare the effectiveness of various control schemes in reducing the orbital sander vibration

1.5 Scope

This work is focused on measuring the input spectrum of the orbital sander in two conditions to determine the dominant vibration axis of the orbital sander. Based on the dominant axis, the experimental modal analysis for the orbital sander is performed. The validation of the frequency response function and the output acceleration between experiment and modeled orbital sander is carried out. The coupled orbital sander-hand-arm model is developed and the comparison between PD and AFC schemes to attenuate the hand-arm vibration for the orbital sander is made.

1.6 Thesis outlines

This thesis is divided into five chapters which are introduction, literature review, methodology, results and discussion, and finally conclusion. Chapter One consists of background study, problem statement, motivation of work, objectives and scope of the research. Chapter Two describes a comprehensive literatures on hand-arm vibration syndrome (HAVs), the guidelines of hand-transmitted vibration, hand-held power tools structure modeling, biodynamic hand-arm models, coupled power tools-hand-arm model and finally hand-arm vibration attenuation methods. Chapter Three presents the methodology of current work and the results are discussed in Chapter Four. Finally, Chapter Five describes the conclusion of this research and recommendation for future work.

CHAPTER 2

LITERATURE REVIEW

2.1 Overview

In this chapter, six main topics are presented as below:

- Hand-arm vibration syndrome (HAVs) and the epidemiological studies
- The guidelines to protect and measure the hand-arm vibration
- Modeling of hand-held power tools
- Human hand-arm biodynamic models
- Coupled power tool-hand-arm models
- Attenuation of hand-transmitted vibration

2.2 Hand-arm vibration syndrome (HAVs) and the epidemiological studies

Prolonged exposure to the hand-transmitted vibration from the power tools may cause hand-arm vibration syndrome (HAVs) which is the combination of vascular and non-vascular disorder in the hand-arm system (Bovenzi, 1998; Mansfield, 2005). The vascular disorder is characterized by Secondary Raynaud's Disease while the non-vascular is represented by Carpal Tunnel Syndrome (CTS) (Bovenzi, 1998; Fridén, 2001; Stoyneva, et al., 2003; Mansfield, 2005; Griffin, et al., 2006).

The most common pathology associated with the vascular disorder of HAVs is Vibration White Finger (VWF). The example of VWF disease is shown in Figure 2.1. In this figure, the symptom of VWF can be identified through the white and pale signs on the human fingers. If the condition is not improved, these symptoms are

extended to be red and painful and at worst can damage the structure of the fingers if there is no necessary action carried out (HSC, 2005; Griffin, et al., 2006).



Figure 2.1: The example of Vibration White Finger (VWF) disease (Hunter, 2011)

Meanwhile, the non-vascular disorder of HAVs is related to osteoarticular and neurological disorder. The pathology of osteoarticular disorder can cause degenerative changes in bones and joints of the wrist and elbow (Griffin, 1990; Bovenzi, 1998) while the neurological disorder can induce the feeling of numbness, tingling and cramps at the human hand (Brammer, et al., 1987; Griffin, et al., 2006).

In previous decades, many researchers and organizations have performed the epidemiological studies of the hand-arm vibration. In Europe, European Communities (2004) revealed that 17 % of their workers are exposed to the machinery and the power tools for not less than half of their working life. Meanwhile, 22 % workers in Spain are exposed to the portable electric and pneumatic tools (Vergara, et al., 2008).

In South Africa, 15 % of the gold miner workers are affected by HAVs due to prolonged exposure of the rock drill (Sampson and Niekerk, 2003; Nyantumbu, et al., 2007). From this percentage, 2 % of them have vascular disorder, 5 % affected by neurological disorder and the rest are involved with both pathologies. The weighted vibration level of the rock drill exceeded 20 m/s^2 as reported by Niekerk, et al.

(1998). Burke, et al. (2005) revealed that 15 % from 26,842 workers in the mining industry suffered with HAVs.

Bovenzi, et al. (2005) carried out epidemiological study on the HAVs effect to the female workers in Italy, where 19 % of the 100 female workers have CTS and 4 % are involved with vascular disorder. The average weighted vibration of the orbital sander is reported to be 7.3 m/s^2 . Neely and Burstrom (2006) found no differences for the threshold measurement between male and female and Bylund (2004) showed that both genders received the same power absorption from the hand-held power tools.

2.3 The guidelines to protect and measure hand-arm vibration

From the previous section, there are various pathology disorders affecting the human hand-arm due to the transmitted vibration from the power tools. In order to protect the human hand-arm from these problems, there are the guidelines and the standards for the measurement of the hand-transmitted vibration.

2.3.1 Guidelines and references for hand-transmitted vibration

In Sweden, National Institute of Working Life (NIWF) (2006) produced the hand-arm vibration database while the Off-highway Plant and Equipment Research Centre (HAVTEC-OPERC) (2006) produced the health and safety study module. Both organizations shared the objectives of measuring the vibration level of hand-held power tools and revealing the effect of HAVs to the workers.

Based on ISO 5439 (2001), Health and Safety Commission (HSC) (2005) and Griffin, et al., (2006) produced the guidelines and hand-arm vibration reference chart for the hand-arm vibration risk assessment. The guidelines improve the previous version which developed by EU in 2002 (HSE, 2005: Nelson and Brereton, 2005).

For the daily vibration exposure $A(8)$, the EU has set the vibration limit values of 2.5 m/s^2 for the Exposure Action Value (EAV) and 5 m/s^2 for the Exposure Limit Value (ELV) (EU, 2002). These limit values are based on eight hours of vibration exposure time. The daily vibration exposure can be calculated by using equation (2.1) (ISO 5349-1, 2001):

$$A(8) = a_{hv} \sqrt{T/T_0} \quad (2.1)$$

where,

a_{hv} = Vibration total value.

T = Total daily vibration exposure.

T_0 = Reference duration of 8 hours.

The workers who are exposed to the vibration must be alert and have to take a necessary action to control the vibration if they exceeded the EAV value and must never reach the ELV limit value (EU, 2002). The detail of the hand-arm vibration reference chart is shown in Appendix A.

2.3.2 Standard measurement of hand-transmitted vibration

There are four main factors which are emphasized when measuring and analyzing the hand-arm vibration; (1) vibration axis, (2) vibration frequency, (3) vibration magnitude and (4) vibration duration (Griffin, 1990; Griffin, et al., 2006). These factors are known to affect the result of hand-transmitted vibration (Mansfield, 2005). Other factors such as hand posture, contact area, push force as well as grip force can also influence the hand-transmitted vibration result. The International Organization of Standardization (ISO) provides the procedures to enable a proper measurement of the hand-transmitted vibration.

The first standard for measurement and assessment of hand-transmitted vibration is produced in 1986 which is the ISO 5349 (1986). This standard is reviewed and replaced fifteen years later by ISO 5349 (2001) (Mansfield, 2005). The new standard consisted of two main parts of the ISO 5349-1 (2001) and ISO 5349-2 (2001). The first part explains the general requirement for measuring hand-transmitted vibration in multi-axis (x , y and z -axis) direction. For the power tool such as orbital sander, the position and coordinate system for the multi-axis vibration measurement at the flat-palm surface is based on Figure 2.2. The figure shows that the coordinate system for the flat-palm surface is covered both biodynamic and basicentric coordinates with the x -axis is pointing downward to the base of the orbital sander, the y -axis is pointing towards the front side of the orbital sander while the z -axis is parallel with the fingers pointing direction.

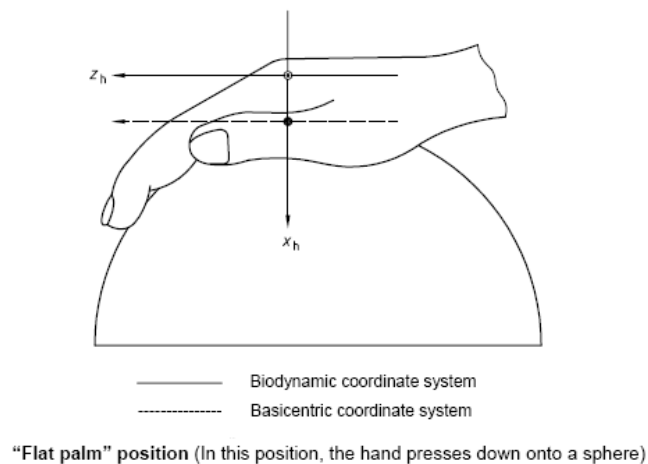


Figure 2.2: Biodynamic and basicentric coordinate system for flat-palm position (ISO 5349-1, 2001)

The first part of ISO 5349 (2001) also define the calculation of the frequency-weighted vibration total value (a_{hv}). This calculation is used for the uniform comparison of measurement. The equation of frequency-weighted vibration total value (a_{hv}) is shown in equation (2.2):

$$a_{hv} = \sqrt{a_{hwx}^2 + a_{hwy}^2 + a_{hwz}^2} \quad (2.2)$$

where a_{hwx} , a_{hwy} and a_{hwz} are the values of frequency-weighted RMS (root mean squares) acceleration for every single axis (x , y and z -axis). The calculation is involved the octave band limitation within 8 - 1000 Hz. The frequency-weighted filter (W_h) for this calculation is shown in Figure 2.3.

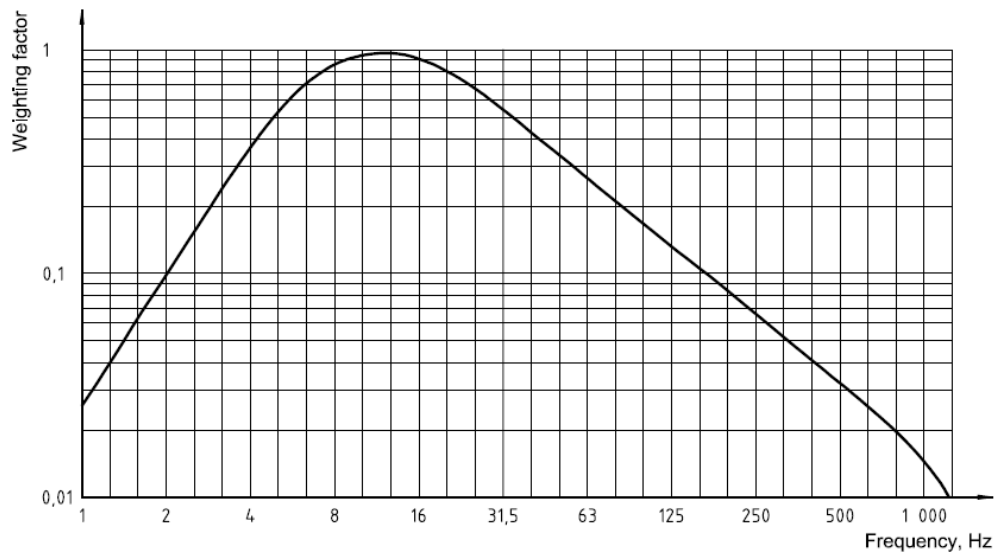


Figure 2.3: Frequency-weighting filter (W_h) with band limitation for hand-transmitted vibration (ISO 5349-1, 2001)

From Figure 2.3, at low frequencies, the weighted factor is high which can be considered to be the most harmful. Meanwhile, the frequencies which are out of this range can be neglected.

In some cases, the estimated total vibration value has to be calculated when the measurement of the three vibration axes cannot be done simultaneously. This calculation can be obtained from the second part of ISO 5349 (2001). Moreover, the ISO 5349-2 (2001) also described the practical measurement guideline such as the mounting of accelerometers, duration of measurement and the working procedures.

2.4 Modeling of hand-held power tools

Oddo, et al., (2004) modeled a suspended handle of the rock drill as a single-degree-of-freedom (SDOF) system to attenuate the hard-arm vibration. Two types of suspended handles are modeled; (1) handle with four helicoidally springs and (2) handle with four viscoelastic mounts. Using the four-pole parameter (Snowdon, 1971), the models are coupled with the four-degree-of-freedom (4DOF) ISO 10068 hand-arm model to observe the effectiveness of the suspended handles.

Golysheva, et al., (2004) developed a dynamic model for the electro-pneumatic hammer consisted of five main parts of the hammer which include the suspended handle, machine casing, exciting piston, striker and the pick. A SDOF hand-arm model is coupled with the suspended handle of the hammer and the hand-arm model parameters are experimentally derived. The details of cross section diagram and dynamic model of the pneumatic hammer are shown in Figure 2.4. The figure shows that the combination of vibration isolation and dynamic absorption principles are used to attenuate the hand-arm vibration for this model.

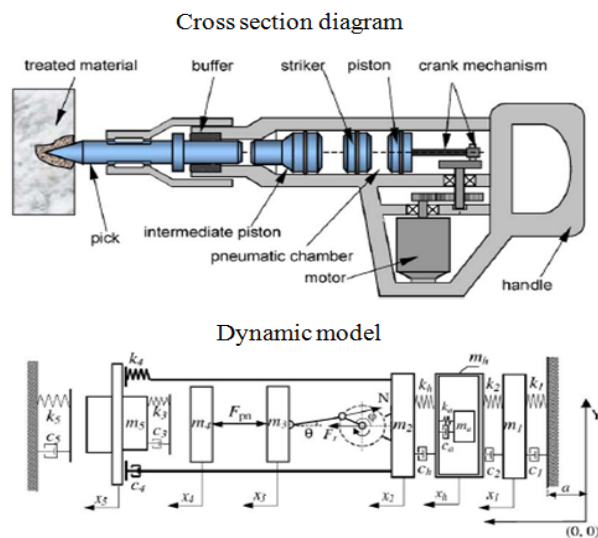


Figure 2.4: Cross section diagram and dynamic model of pneumatic hammer (Golysheva, et al., 2004)

2.5 Human hand-arm biodynamic models

The biodynamic hand-arm model is used to observe the dynamic behavior and response of the hand-arm system such as motion and force (Dong, et al., 2005). There are different types of human hand-arm biodynamic models in order to measure and evaluate the response of the hand-arm system as well as to perform the risk assessment and the vibration suppression mechanism of the hand-arm system (Rakheja, et al., 2002).

Basically, human hand-arm biodynamic models are categorized into two different types which is to-the-hand and through-the-hand biodynamic models. To-the-hand biodynamic model is usually used to investigate the driving-point mechanical impedance (DPMI) of the hand-arm system while through-the-hand model is used to evaluate the transmitted vibration in specific hand-arm segments (Rakheja, et al., 2002).

2.5.1 To-the-hand biodynamic models

As mentioned previously, the DPMI can be defined as the ratio of the applied input force $F(s)$ to the resulting velocity $\dot{X}(s)$ at the hand-handle interface. The equation of DPMI is given by equation (2.3):

$$Z_D(s) = F(s) / \dot{X}(s) \quad (2.3)$$

where $(s = j\omega)$ is a complex numbers that can be expressed in terms of magnitude and phase. Rakheja, et al., (2002) carried out a comprehensive literature review on the biodynamic hand-arm models from single-degree-of-freedom (SDOF) to multi-degree-of-freedom (MDOF) models, lumped mass approximated models and distributed parameter models.

The first hand-arm beam model is developed by Wood, et al., in 1978. This model is presented as two long bones of the arm by using distributed mass and stiffness parameters. The next hand-arm beam model is produced in ISO 10068 (1998). In 1972, the first SDOF hand-arm model is developed by Reynolds and Soedel covers all three orthogonal axes directions. Miwa, et al. (1979) designed a higher degree-of-freedom of the hand-arm models including 2DOF and 3DOF of semi-defined hand-arm models. Rakheja, et al., (2002) reported that some researchers have developed 3DOF and 4DOF hand-arm models between 1977 to 1998 such as Mishoes and Suggs, (1977), Reynolds and Falkenberg, (1984), Daikoku and Ishikawa, (1990), Gurram, (1993) and ISO 10068, (1998).

Since the measurement methods are not standardized plus the different conditions of DPMI measurement (Rakheja, et al., 2002), the result of parameters obtained for each hand-arm model are significantly different (Gurram, et al., 1995; Dong, et al., 2005). As a result, most of the biodynamic hand-arm models are not suitable for the advance modeling of coupled hand-arm with the power tools (Rakheja, et al., 2002). For example, some of the natural frequencies obtained for the hand-arm model are significantly low and did not coincided with the formulated frequency range. Also, there are no specific ranges of frequency for the model parameters in each axis. These problems mostly occurred for the higher degree of freedom hand-arm models such as Reynolds and Falkenberg, (1984), Daikoku and Ishikawa, (1990), Gurram, (1993) and ISO 10068, (1998). There are three models; Reynolds and Soedel, (1972), Mishoe and Suggs, (1977) and Miwa, et. al. (1979), which have obtained all the natural frequencies in the range of formulated frequency and only Reynolds and Soedel specified the range of frequency for each direction of the hand-arm model parameters.

2.5.2 Through-the-hand biodynamic models

Transmissibility principle played a main role in developing through-the-hand biodynamic model (Rakheja, et al., 2002). Transmissibility $T(s)$ is defined as a ratio measurement of resulting acceleration $\ddot{X}(s)$, velocity $\dot{X}(s)$ or displacement $X(s)$ to the excitation acceleration $\ddot{X}_0(s)$, velocity $\dot{X}_0(s)$ or displacement $X_0(s)$ and can be calculated using equation (2.4):

$$T(s) = \ddot{X}(s) / \ddot{X}_0(s) = \dot{X}(s) / \dot{X}_0(s) = X(s) / X_0(s) \quad (2.4)$$

Since the transmitted vibration data is not very satisfactory plus the difficult process of obtaining the model parameters, the application of through-the-hand models in determining the biodynamic response of the hand-arm system is unpopular (Cherian, et al., 1996; Rakheja, et al., 2002).

Cherian, et al., (1996) developed a five-degree-of-freedom (5DOF) hand-arm model to investigate the transmitted vibration at specific segments of the hand-arm system. The system consisted of three main parts of the hand, forearm and upper arm. A 25 N of grip force is applied at the palm of the orbital sander during the experiment with the frequency range formulated from 10 to 200 Hz. In this study, the model parameters are obtained from the vibration transmissibility characteristic result.

2.6 Coupled power tool-hand-arm models

Literatures on the DPMI cover the influence of the grip and push forces, handle sizes, hand postures and vibration directions of the biodynamic hand-arm (Aldien, et al., 2005; Marcotte, et al., 2005; Aldien, et al., 2006; Besa, et al., 2007, Xu, et al., 2011; Adewusi et al., 2012). However, there are only limited studies on

the dynamic behavior of coupled power tool-hand-arm model using the DPMI result of the biodynamic hand-arm model.

An example of the use of the to-the-hand biodynamic model is carried out by Oddo, et al., (2004), which involved the application of ISO 10068 (4DOF) second biodynamic hand-arm model coupled with modeled suspended handle of the rock drill using the four-pole parameters theory. The natural frequency range used for the drill is between 35 to 45 Hz which is in the range of formulated frequency (10-500 Hz) of the ISO 10068 hand-arm model. For the 50 N push force, the measured and computed result showed good correlation for the frequency range of 50 - 400 Hz. This result proves that ISO 10068 hand-arm model is acceptable to be used in the study.

Ko, (2008) developed coupled orbital sander-hand-arm model by using the 5DOF through-the-hand biodynamic model which have been developed previously by Cherian, et al., (1996). In this study, the elastomeric pad is used as an intercession material between the orbital sander and the hand-arm model to attenuate the vibration transmitted to the hand-arm system. The result shows that the elastomeric pad is better than flow divider developed by Cherian, et al., in attenuating the vibration transmitted to the hand-arm system.

2.7 Attenuation of hand-transmitted vibration

There are several ways of reducing the vibration level transmitted to the hand. The best method is to control vibration from the source which involved the masses balancing, translating or rotating, clearance minimization and streamlining the disturbances exposed components (William, 2007). For example, in the commercial

hand-held power tool manufacturer, Makita, (2012b) managed to dynamically balance the motor of the electric jigsaw which resulted in 40 % reduction of vibration.

In addition, redesign the structure of the tool can shift the natural frequency of the tool away from the operating frequency. As a result, it can reduce the vibration and avoid the resonance of the structure (William, 2007). For example, Greenslade and Larsson (1997) redesigned the chainsaw used by the lumberjack. The result shows that the vibration is reduced by 85 % (Sampson and Niekerk, 2003). Even though this solution is good, it requires structure redesign and increasing tool components which contributed to the design complexity and increasing overall cost of the tools (Golysheva, et al., 2004; Ko, 2008). However, it is depend on how the components will be designed. As such for the aftermarket demand, the remaining solution is to go for the vibration isolation approach, vibration absorption approach and active vibration control technology (Golysheva, et al., 2004; Hassan, et al., 2010).

2.7.1 Vibration isolation approaches

Vibration isolation approach involved the use of isolator which can be placed between the sources (power tools) and the receivers (human hand). Isolator consisted of stiffness and damping element which in general is made of rubber, elastomeric and viscoelastic materials. By using these elements, the transmitted vibration from the sources to the hand-arm system can be reduced (William, 2007).

A rubber mount is usually used as an isolator for most of the tools since it is compact, cost effective and maintenance free (Tewari and Dewangan, 2009). Ko, et al., (2011a) designed three types of suspended handle for the portable petrol grass trimmer. In these designs, a rubber mount is used as an isolator between the base plate and the suspended handle. The material of the handles and distance of the

rubber mount are different for each type of suspended handle. The result shows that the handle with heavier material can reduce the transmitted vibration by 76 %. The study also proved that the distance of rubber mount influenced the reduction of the vibration.

Anti vibration glove is another vibration isolation approach usually used for the hand-held power tools as shown in Figure 2.5. In this figure, anti-vibration glove is used to attenuate the hand-transmitted vibration when using the orbital sander. There are various anti-vibration gloves which are priced from USD 8 for a simple padded glove lined with viscolas VEP padding to the more expensive gloves of USD 30 for glove with patented air technology, full finger synthetic leather, anti-vibration mechanic air glove and fulfilled the ANSI and ISO 10819 requirement (The Man Store, 2012).



Figure 2.5: Anti-vibration glove used to attenuate hand-arm vibration when using the orbital sander (Lee Valley, 2012)

Several studies have been carried out to investigate the effectiveness of using the anti-vibration glove. Sampson and Niekerk (2003) revealed that most of the anti-vibration gloves available in the market are not effective at low frequency and restrict the dexterity of the fingers. There are also the inconvenient feeling when using the thick glove which can cause aches and pains at the hand due to the extra

forces required to hold the tools. Moreover, Dong, et al., (2005) claimed that anti-vibration glove only reduce the vibration at the handle of the power tools but not on the fingers.

For the power tools such as angle grinders, Bosch has developed anti-vibration handle which is priced at USD 24 (Toolnweld, 2006). The anti-vibration handle works on the isolation effect when damping element is inserted between the handle and the motor housing with the damping element frequency characteristics tuned to match the characteristics of the motor. The magnitude of isolation has achieved however is not mentioned. An almost similar design is developed by Makita, (2012a) for angle grinder which is called anti-vibration side handle as shown in Figure 2.6. In this figure, the handle works on the basis of isolation where the elastomeric components (rubber damper) are inserted to isolate the handle from the vibration of the body of the power tools.

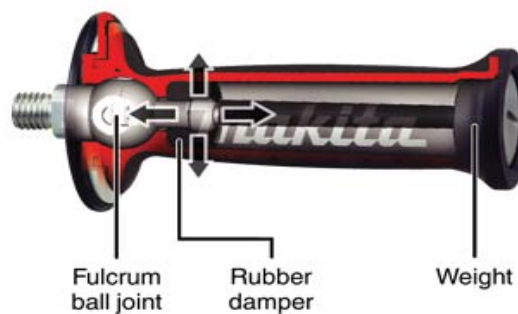


Figure 2.6: Anti-vibration side handle (Makita, 2012a)

2.7.2 Vibration absorption approaches

The vibration of power tools can be reduced by attaching a secondary mass or in some cases with a stiffness elements at the source or receiver of the power tools such as dynamic vibration absorber (DVA) (Golysheva, et al., 2004; Ko, et al., 2011b). The natural frequency of DVA is tuned to match the natural frequency of the

main mass. As a result, the energy of the main mass will be absorbed by the DVA and the motion at the natural frequency of the main mass can be reduced to zero (William, 2007).

Ko, et al., (2011b) designed a tuned vibration absorber (TVA) and attached to the electric grass trimmer to reduce the hand-transmitted vibration. The TVA is attached at the various shaft location of the grass trimmer. The experiment is carried out in two field conditions for cutting and no cutting operations. The result shows that the vibration at the handle of the grass trimmer is significantly reduced in z -axis direction for both conditions. Also, the TVA produced the best performance by reducing the vibration by 95 % for the grass trimmer. The same concept has been applied before by Strydom (2000), where the DVA is attached to the handle of rock drill and the result shows that the vibration reduced by 40 %.

One approach of applying the dynamic vibration absorber on the receiver is done by Cherian, et al, (1996) which is named as flow divider. The flow divider is attached to the five-degree-of-freedom (5DOF) of hand-arm model consisted of the hand, forearm and upper arm. The result shows that the vibration level at the hand is reduced to 5.3 m/s^2 from the original weighted acceleration of 6.8 m/s^2 . However, due to the characteristic of the DVA, the vibration level at the upper arm and forearm has increased by 10 % and 13 % respectively. Rade and Steffen, (2002) revealed that the vibration level at certain points can be increased or decreased depend on the DVA characteristic.

2.7.3 Active vibration control (AVC) approaches

For cases where the disturbances and frequencies of the dynamic system are changing with time, passive control becomes ineffective. Due to this condition, an

active vibration control (AVC) is introduced to the system (William, 2007; Hassan, et al., 2010). Figure 2.7 shows the basic control diagram of the AVC system. In this figure, the AVC system consisted of sensor to measure the feedback signal of the system (process) and a set of control system to process the feedback signal and computed the difference signal for the actuator to counteract the forces produced by the system (Mohamad, 2004; William, 2007). Basically, the actuator such as piezoelectric, electric motor and hydraulic cylinder are used in the AVC system (William, 2007).

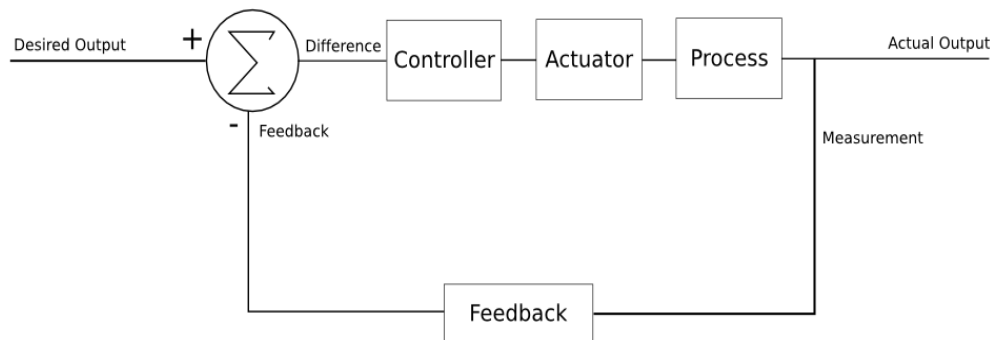


Figure 2.7: Basic control diagram for AVC system (Stienecker, 2011)

There are many controller techniques that can be applied in the AVC system. One of the techniques which has been widely used in the AVC field is the proportional-integral-derivative (PID) (Yildirim, 2004; Hassan, et al., 2010). The theory and details of PID technique are discussed later in Chapter Three (Methodology).

There are many applications of using PID controller in the experiment as well as in simulation works. For example, Trojanowski and Wiciak, (2009) applied the PID controller scheme to suppress the vibration of the aluminium plate. In this experiment, the plate is clamped in one side with the other side is freely vibrated. Five piezoelectric elements are introduced to the plate with four of them functioned

as a sensor and actuator. Meanwhile, another one is used to produce an excitation for the plate. The result shows that the piezo actuator can suppress 22.5% to 25% of vibration for both measured locations.

A similar study is carried out by Knot, et al., (2011) which involved simulation using PID technique as a controller for the cantilever beam and piezoelectric elements as the sensor and actuator. The cantilever beam is modeled in the finite element (FE) environment (Ansys) and then constructed in the Simulink software for the AVC simulation. Two types of models are designed which is named as full and reduced models. The result shows that both models have achieved the reduction of the vibration of the cantilever beam.

The application of PID controller at the plate is extended by Rahman, et al., (2011). The study is focused on using one of the PID control elements which is proportional (P) gain. The P gain is used as a controller parameter to suppress the vibration of the flexible plate. In this experiment, piezoelectric patch is used as an actuator for the AVC system. The first five natural frequencies of the plate are defined and the result shows that the P gain controller has reduced most plate energy at the fourth natural frequency with 15.5 % of vibration reduction.

Apart from PID controller, there are many types of controller techniques which can be applied in the AVC field such as neural network (NN) (Yildirim, 2004), fuzzy logic (FL) (Li, et al., 2009; Ahmad, et al., 2010), genetic algorithm (GA) (Bruant, et al., 2010), Linear Quadratic Gaussian (LQG) (Chen, et al., 2003; Waghulde, et al., 2010) and etc. In the commercial hand-held power tool manufacturer, Bosch, (2012) claimed that AVC has been successfully implemented in their rotary hammer drill product. However, the design of the AVC system and the magnitude of vibration reduction are not mentioned.

2.7.3.1 Active Force Control (AFC) technique

One of the most efficient control technique in the AVC field is called active force control (AFC). AFC is firstly introduced in 1981 by Hewit and Burdess. After that, many researchers have applied the AFC technique in their application and the results proved that the technique is effective for the AVC system even though in the influence of known or unknown disturbances (Mailah, et al., 2009; Hassan, et al., 2010). The discussion of theory and the detailed process of AFC control technique are covered in Chapter Three (Methodology).

Kwek, et al., (2003) applied the AFC technique to control the five-link biped robot. The robot is tested for the biped walk on the horizontal flat surface and the locomotion is set to be constrained within the sagittal plane. Three types of control schemes are applied which include the PD, AFC with crude approximation (AFC-CA) and AFC with iterative learning method (AFC-ILM). The results show that both AFC schemes produced a superior result than PD scheme even though under the presence of disturbances.

Varatharajoo, et al., (2011) incorporated the AFC technique in two-degree-of-freedom (2DOF) spacecraft attitude controller. Two types of controllers are introduced to the system which is PD and PD+AFC techniques. The numerical analysis is performed and the best result is obtained by PD+AFC controller. The AFC technique also improved the accuracy of attitude pointing of the Combined Energy and Attitude Control System (CEACS).

There are very limited literatures on the application of AFC technique for the hand-held power tools. Hassan, et al., (2010) applied the AFC control technique to suppress the vibration at the rear handle of hedge trimmer. The simulation consisted

of applying four types of controllers which is PID, AFC with crude approximation (AFC-CA), AFC with fuzzy logic (AFC-FL) and AFC with iterative learning method (AFC-ILM). The external disturbance is introduced to the system and the performances of the controllers are compared. The result proved that all three types of AFC schemes produced a better result compared to PID controller with the AFC-FL scheme gives the best performance.

One approach of applying the AFC technique on the receiver is carried out by Mailah, et al., (2009). The AFC controller is constructed and linked with the model of two-link planar mechanical manipulator that represented a human arm. An excitation is applied to the certain point of the human arm model to evaluate the effect when performing trajectory tracking task in two dimensional spaces. The result shows that AFC scheme is better than PD scheme in suppressing the vibration and can produce an accurate tracking performance for the system.

2.8 Discussion

From the literatures, it is realized that prolonged exposure to the hand-transmitted vibration from the power tools can result of hand-arm vibration syndrome (HAVs) which is the combination of vascular and non-vascular disorder (Brammer, et al., 1987; Griffin, 1990; Bovenzi, 1998; Fridén, 2001; Stoyneva, et al., 2003; HSC, 2005; Mansfield, 2005; Griffin, et al., 2006). Epidemiology studies have come out with a statistical data to prove that the power tools can contribute to the HAVs (Niekerk, et al., 1998; Sampson and Niekerk, 2003; Bylund, 2004; European Communities, 2004; Bovenzi, et al., 2005; Burke, et al., 2005; Neely and Burstrom, 2006; Nyantumbu, et al., 2007; Vergara, et al., 2008).